

Inferring ozone production in an urban atmosphere using measurements of peroxyxynitric acid

K. M. Spencer¹, D. C. McCabe^{2,*}, J. D. Crouse¹, J. R. Olson³, J. H. Crawford³, A. J. Weinheimer⁴, D. J. Knapp⁴, D. D. Montzka⁴, C. A. Cantrell⁴, R. S. Hornbrook⁴, R. L. Mauldin III⁴, and P. O. Wennberg^{2,5}

¹Division of Chemistry and Chemical Engineering, California Institute of Technology, Pasadena, CA, USA

²Division of Geological and Planetary Sciences, California Institute of Technology, Pasadena, CA, USA

³NASA Langley Research Center, Hampton, VA, USA

⁴National Center for Atmospheric Research, Boulder, CO, USA

⁵Division of Engineering and Applied Science, California Institute of Technology, Pasadena, CA, USA

*current address: AAAS Science & Technology Policy Fellow, United States Environmental Protection Agency, Washington, DC, USA

Received: 1 December 2008 – Published in Atmos. Chem. Phys. Discuss.: 28 January 2009

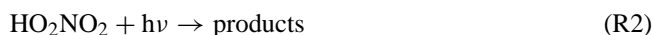
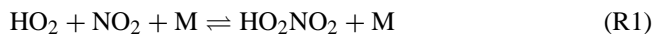
Revised: 28 April 2009 – Accepted: 15 May 2009 – Published: 8 June 2009

Abstract. Observations of peroxyxynitric acid (HO_2NO_2) obtained simultaneously with those of NO and NO_2 provide a sensitive measure of the ozone photochemical production rate. We illustrate this technique for constraining the ozone production rate with observations obtained from the NCAR C-130 aircraft platform during the Megacity Initiative: Local and Global Research Observations (MILAGRO) intensive in Mexico during the spring of 2006. Sensitive and selective measurements of HO_2NO_2 were made in situ using chemical ionization mass spectrometry (CIMS). Observations were compared to modeled HO_2NO_2 concentrations obtained from the NASA Langley highly-constrained photochemical time-dependent box model. The median observed-to-calculated ratio of HO_2NO_2 is 1.18. At NO_x levels greater than 15 ppbv, the photochemical box model underpredicts observations with an observed-to-calculated ratio of HO_2NO_2 of 1.57. As a result, we find that at high NO_x , the ozone production rate calculated using measured HO_2NO_2 is faster than predicted using accepted photochemistry. Inclusion of an additional HO_x source from the reaction of excited state NO_2 with H_2O or reduction in the rate constant of the reaction of OH with NO_2 improves the agreement.

1 Introduction

Peroxyxynitric acid, HO_2NO_2 , is an important reservoir of both HO_x ($\text{HO}_x = \text{OH} + \text{HO}_2$) and NO_x ($\text{NO}_x = \text{NO} + \text{NO}_2$) radicals. These radicals are of primary atmospheric importance as they influence the production and degradation of tropospheric ozone and numerous volatile organic compounds (Murphy et al., 2004). Ozone production in urban environments is initiated by OH radicals and requires sunlight, NO_x , and hydrocarbons. The relative amounts of these species control the rate of ozone production (Seinfeld and Pandis, 2006).

The only known pathway for the formation of HO_2NO_2 in the atmosphere is the association reaction of HO_2 and NO_2 , Reaction (R1) (Niki et al., 1977). HO_2NO_2 is lost via thermal decomposition, Reaction (R1) (Graham et al., 1977, 1978; Zabel et al., 1995; Gierczak et al., 2005); UV and visible/near-IR photolysis, Reaction (R2) (Macleod et al., 1988; Roehl et al., 2002; Knight et al., 2002); and reaction with the OH radical, Reaction (R3) (Trevor et al., 1982; Smith et al., 1984; Barnes et al., 1986; Jimenez et al., 2004).



The relative importance of the HO_2NO_2 sinks depends on temperature, pressure, OH radical concentration, and the



Correspondence to: K. M. Spencer
(kspencer@caltech.edu)

UV/IR radiation field. The lifetime of HO₂NO₂ with respect to thermal decomposition varies due to the strong temperature dependence of this process (Kim et al., 2007). As temperature decreases, loss due to photolysis and reaction with OH radical become increasingly important. At altitudes greater than 7 km, photolysis and reaction with OH become the dominant loss mechanisms (Roehl et al., 2002). The formation of HO₂NO₂ followed by its loss via reaction with OH forms a NO_x-catalyzed sink of HO_x radicals (Roehl et al., 2002).

The role of HO₂NO₂ in photochemistry of the lower troposphere has been less explored, in part because of a paucity of observations of this compound. In situ measurements of HO₂NO₂ have been obtained previously in the free troposphere during the 2004 INTEX-NA campaign (Kim et al., 2007) and in Antarctica (Slusher et al., 2001). An indirect estimate of the HO₂NO₂ abundance was obtained from the sum of peroxyxynitrate observations during the 2000 TOPSE campaign (Murphy et al., 2004).

Here, we present in situ measurements of HO₂NO₂ in and around Mexico City. These measurements were made in March of 2006 from the NCAR C-130 aircraft platform during the MILAGRO field experiment. One goal of the MILAGRO mission, and the focus of the C-130 flights, was to investigate the processing and outflow of pollution from Mexico City. Most flights occurred during the daytime hours at altitudes below 7 km and temperatures between 260 and 300 K. The majority of the data are between 270 and 283 K. This study is limited to six of the MILAGRO flights (8, 22, 23, 26, 28, and 29 March) during which all necessary species were measured. A photochemical steady-state approximation of HO₂NO₂ under MILAGRO conditions is discussed, and measured HO₂NO₂ concentrations are compared to those predicted by the NASA LaRC box model. A simplified method of estimating the rate of ozone production using HO₂NO₂ is compared to full NASA LaRC box model calculations of the rate of ozone production.

2 Method

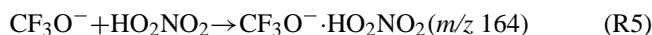
2.1 Instrumentation

NO and NO₂ mixing ratios were measured by photofragmentation/chemiluminescence. The precision of these measurements is ~15 pptv and the overall uncertainties are ±(15+7% of the mixing ratio) pptv and ±(15+10% of the mixing ratio) pptv, respectively (Campos et al., 1998; Weinheimer et al., 1998). CH₂O mixing ratios were measured by tunable diode laser absorption spectroscopy with an uncertainty of 15% (Fried et al., 2003; Wert et al., 2003). HO₂ mixing ratios were determined by chemical-conversion/chemical ionization mass spectroscopy with an uncertainty of 35% (Cantrell et al., 2003). Non-methane hydrocarbons (NMHC) were measured using whole air sampling (WAS) and subse-

quent analysis was conducted by gas chromatography/mass spectrometry/flame ionization detection/electron capture detection (Colman et al., 2001; Blake et al., 2003). H₂O mixing ratios were calculated using the ambient water vapor pressure and corrected static pressure. These measurements and the ambient temperature measurements are included in the NCAR C-130 standard airborne scientific measurements and are discussed in RAF Bulletin No. 9 (Miller and Friesen, 1985). The full details of measurements taken during MILAGRO from the NCAR C-130 aircraft platform can be found at <http://mirage-mex.acd.ucar.edu/Measurements/C130/index.shtml>.

HO₂NO₂ measurements were made using the Caltech chemical ionization mass spectrometry (CIMS) instrument. The instrument has been described in detail previously by Crouse et al. (2006). Briefly, the Caltech CIMS consists of a flow tube controlled at 35 mbar total pressure where a reagent ion, CF₃O⁻, interacts with ambient air diluted 1:4 with dry nitrogen. Ions are sampled from the flow tube into a quadrupole mass filter and detected with a channel electron multiplier. Each mass-to-charge ratio is observed for ~0.5 s. HO₂NO₂ masses were monitored every ~15 s.

Negative ion chemistry of CF₃O⁻ has been shown to provide sensitive and selective detection of many inorganic and organic acids (Huey et al., 1996; Amelynck et al., 2000a,b; Crouse et al., 2006) and was exploited in this work to detect HO₂NO₂. The reaction of CF₃O⁻ with acids follows several pathways. Reaction with strong acids proceeds via fluoride ion transfer (Huey et al., 1996) while reaction with weaker acids yields clusters of reagent ion and analyte (Amelynck et al., 2000a). HO₂NO₂ reacts with CF₃O⁻ via fluoride ion transfer through Reaction (R4), clustering through Reaction (R5) (Crouse et al., 2006), and HF elimination through Reaction (R6), providing three distinct ion signals. Reactions (R4–R6) are complicated by competing reactions with CF₃O⁻ water cluster (CF₃O⁻ · H₂O).

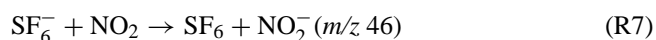


2.1.1 Sensitivity and calibration

Due to differences in reactivity of CF₃O⁻ and its water cluster, the sensitivity of the CIMS instrument to the ion products of the three channels, Reactions (R4, R5, R6), is dependent on the mixing ratio of water vapor in the flow tube (Crouse et al., 2006). This dependence is quantified via laboratory measurements. A small quantity of HO₂NO₂ was introduced into the flow tube. The flow tube humidity was controlled using mass flow controllers to adjust the ratio of air saturated with water vapor to dry zero air. Humidity was quantified by Fourier Transform Infrared (FTIR) spectroscopy using HITRAN line lists (Rothman et al., 2005) and the commercial

spectral manipulation software package GRAMS (Galactic Industries Inc.). The sensitivity of the instrument to the fluoride ion transfer and cluster channels of HO₂NO₂ as a function of H₂O mixing ratio in the flow tube was determined and is presented in Fig. 1. Sensitivity is expressed in ion counts, normalized by the ion counts of the +1 isotopes of the reagent ions, ¹³CF₃O⁻ and ¹³CF₃O⁻ · H₂O, per pptv of HO₂NO₂. The yield of Reaction (R6) is typically one-third that of Reaction (R5). Due to the low reaction yield, Reaction (R6) is not used to quantify the ambient observations of HO₂NO₂.

During calibration, the concentration of HO₂NO₂ in the flow tube was determined by thermally decomposing the HO₂NO₂ into NO₂, Reaction (R1), and quantifying the resultant NO₂ using CIMS with SF₆⁻ as the reagent ion through Reaction (R7) (Huey et al., 1995):



NO₂ is not detected with high sensitivity using CF₃O⁻.

Synthesis of HO₂NO₂ was performed offline using the procedure described in Roehl et al. (2002); gas-phase HO₂NO₂ was produced by flowing dry N₂ over the solution of HO₂NO₂. A small portion of this flow was directed through a critical orifice into a PTFE three-way valve, which directed the flow through either a heated or unheated glass inlet tube (6 mm OD). The heated inlet tube was kept at 190°C, a temperature at which 99.8% of the HO₂NO₂ decomposed, as determined by monitoring the signal with CF₃O⁻ at *m/z* 98. The unheated inlet was maintained at room temperature. The sensitivity of the CIMS to NO₂ was quantified using a dilute mixture of NO₂ in N₂; the concentration of NO₂ in this mixture was quantified with FTIR using HITRAN line lists (Rothman et al., 2005) and the commercial spectral manipulation software package GRAMS (Galactic Industries Inc.).

The CIMS sensitivity to HO₂NO₂ was determined by back-to-back measurements of the products of Reactions (R4), (R5), and (R7). HO₂NO₂ was added through the room temperature inlet and measured using CF₃O⁻ as the reagent ion. Next, HO₂NO₂ was added through the heated inlet and NO₂ was measured using SF₆⁻ as the reagent ion through Reaction (R7). Background NO₂ from NO₂ impurity in the HO₂NO₂ solution was measured using SF₆⁻ by passing the HO₂NO₂ through the room temperature inlet; this background signal was subtracted from the NO₂ signal when the heated inlet was used. The signals from Reactions (R4) and (R5) obtained using the room temperature inlet were also corrected for the small amount of HO₂NO₂ that did not dissociate in the heated inlet and other backgrounds (see below) by monitoring those masses using CF₃O⁻ as the reagent ion with the heated inlet in use. This procedure was repeated at a number of humidities to obtain water-dependent calibration functions for each ion product. Post-mission laboratory calibrations for HO₂NO₂ were conducted. During flight, isotopically labeled HNO₃ was periodically added to

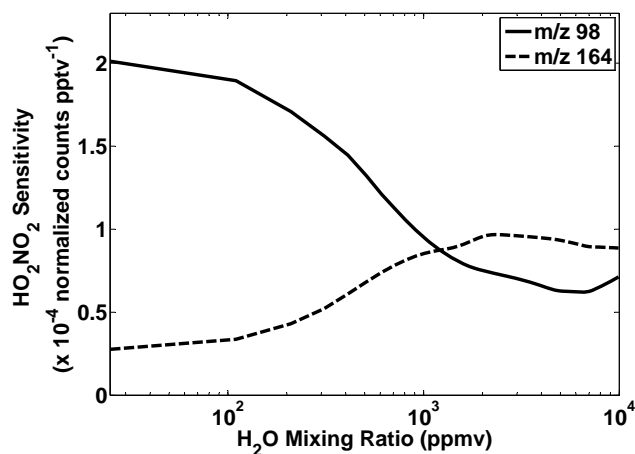


Fig. 1. Sensitivity curves for *m/z* 98 (solid) and *m/z* 164 (dash) as a function of H₂O mixing ratio in the flow tube. The sensitivity curves are used to calculate the final mixing ratios of HO₂NO₂.

the flow tube to monitor the stability of the instrument sensitivity. Sensitivity of the instrument to HNO₃ was consistent and comparable during flight and laboratory calibrations indicating the sensitivity of the instrument to HO₂NO₂ was consistent.

In the absence of HO₂NO₂, ion signals at *m/z* 98 and *m/z* 164 are non-zero, and these background signals must be accounted for in the data analysis. These background signals were measured during flight by periodically passing ambient air through a filter consisting of alumina pellets coated with palladium and nylon wool coated with sodium bicarbonate, quantitatively removing HO₂NO₂. This technique is described in Crouse et al. (2006).

2.1.2 Ambient HO₂NO₂ concentration

HO₂NO₂ concentrations are calculated from the signals observed at *m/z* 98 and *m/z* 164 after normalization by the amount of reagent ion signal, subtraction of background signals, and application of the appropriate sensitivity factor for HO₂NO₂.

Acetate in the form HF · CH₃C(O)O⁻ · H₂O is a known interference in the *m/z* 98 signal. HF · CH₃C(O)O⁻ · H₂O is seen at *m/z* 97, with approximately 2.5% of the *m/z* 97 signal appearing at *m/z* 98 due to heavy isotopes of the ion. Because the *m/z* 97 signal was not monitored during these flights, the interference at *m/z* 98 was estimated from the monitored signal of the acetate-fluoride transfer ion (HF · CH₃C(O)O⁻) at *m/z* 79 and ambient water levels, using a function derived through post-mission laboratory measurements. There are no interferences of which we are aware at *m/z* 164. Background signals were measured (as described above) about every 15 min and are used to model background levels during the flight.

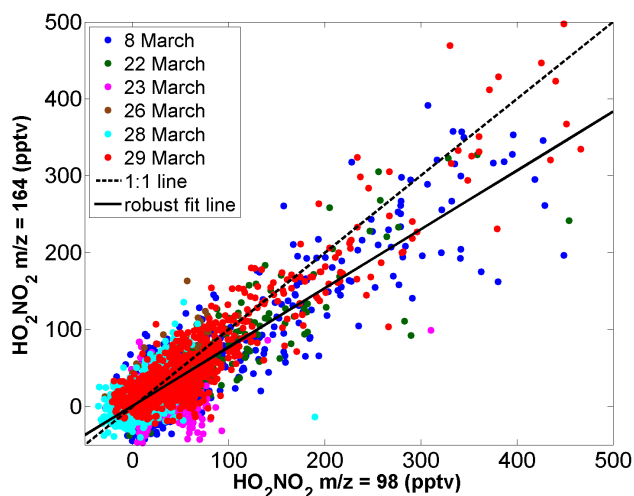


Fig. 2. HO₂NO₂ is measured with two ions: products of fluoride transfer ($m/z=98$) and clustering ($m/z=164$). The data are colored by flight date. The data shown are observations obtained when the measured NO_y differs by less than 10% between m/z 98 and m/z 164 sampling times. The slope of the robust fit line is 0.76; the intercept is 0.90 pptv; $R^2=0.94$. Independent measurements of HO₂NO₂ from these two ions agree very well, indicating that these masses are selective to HO₂NO₂.

A scatter plot of the independent determinations of HO₂NO₂ calculated from the m/z 98 and the m/z 164 signals is shown in Fig. 2. During the flight, there is an ~ 8 s delay between a m/z 98 measurement and the corresponding m/z 164 measurement. Only observations obtained when the measured NO_y differs by less than 10% between m/z 98 and m/z 164 sampling times are included in Fig. 2. The slope of the robust fit line (DuMouchel and O'Brien, 1989; Street et al., 1988) is 0.76; intercept is 0.90 pptv; $R^2=0.94$. These independent measurements are in good agreement, providing confidence in the use of this ion chemistry to quantify HO₂NO₂.

The concentration of HO₂NO₂ used in the subsequent analysis is determined by combining the independent measurements from m/z 98 and m/z 164 as follows. When the water mixing ratio in the flow tube is less than or equal to 200 ppmv, the m/z 98 measurement is used because the sensitivity at m/z 164 is low (Fig. 1; recall that the ambient air pulled into the flow tube is diluted 1:4 with dry N₂). When the water mixing ratio in the flow tube is between 200 to 500 ppmv, the mean of the m/z 98 and the m/z 164 measurements is used. At water vapor mixing ratios greater than 500 ppmv, the m/z 164 measurement is used exclusively. Although the sensitivity is somewhat lower at m/z 164 than at m/z 98 for water mixing ratios between 500 to 1000 ppmv, higher backgrounds and interference from acetate at m/z 98 make the cluster ion (m/z 164) a more robust measure of HO₂NO₂ at these higher water mixing ratios.

The uncertainty in the PNA measurements is approximately $\pm(30\%+30$ pptv). The uncertainty reflects the sum of the precision of the data determined by the counting statistics of the ions, the variability of the background signal, and the uncertainty of the sensitivities shown in Fig. 1.

2.2 Photochemical time-dependent box model

Calculated concentrations of HO₂, NO₂, and HO₂NO₂ and rates of ozone production were obtained from a highly-constrained photochemical time-dependent box model (NASA Langley Research Center (LaRC) box model) (Olson et al., 2006). The modeling approach used is based on the assumption of a diurnal equilibrium (Olson et al., 2006, 2004; Frost et al., 2002; Jaegle et al., 2000). Model inputs include observations of atmospheric parameters such as temperature, pressure, water vapor, and critical long-lived chemical precursor species (O₃, CO, NO, CH₄, non-methane hydrocarbons, acetone). With the exception of NO and the radiation field, the atmospheric state is held constant throughout the model run. NO varies diurnally; however reactive nitrogen, NO_y=NO+NO₂+NO₃+2N₂O₅+HONO+HO₂NO₂, is held constant with partitioning as determined by the model. The amount of total reactive nitrogen is determined so that NO matches the observed value at the time of the measurement. Additional constraints are implemented if data are available. These additional constraints include methanol, ethanol, H₂O₂, CH₃OOH, HNO₃, PAN, acetic acid, and formic acid. Concentrations of these species are computed by the model when data are unavailable. While a discrepancy between calculated and observed values of acetaldehyde (CH₃CHO) does exist and has the potential to impact HO_x levels, constraining the model to observed CH₃CHO values suggests that this uncertainty propagates to impact OH mixing ratios by 5–10% and HO₂ mixing ratios by less than a few percent.

The model chemistry includes HO_x–NO_x–CH₄ gas phase reactions based on the recommendations of Atkinson et al. (2004) and Sander et al. (2003). In addition, the model uses the rate for O(¹D) quenching by N₂ suggested by Ravishankara et al. (2002), temperature dependent quantum yields for acetone photolysis from Arnold et al. (2005), and the parameterization for near-IR photolysis of HO₂NO₂ described by Roehl et al. (2002). Nonmethane hydrocarbon chemistry is based on the condensed mechanism of Lurmann et al. (1986) with modifications included to address remote low-NO_x conditions. Explicit chemistry is included for C₂H₆, C₃H₈, C₂H₄, isoprene, and benzene. C₄ and higher alkanes are lumped together, as are C₃ and higher alkenes, and aromatics other than benzene. Reactions of lumped C₃ and higher alkenes are assumed to be predominantly propene. The assumed aldehyde product is CH₃CHO and reaction rates are based on those for propene. Photolysis rate coefficients are based on spectroradiometer measurements (Shetter and Muller, 1999). The diurnal profiles of the photolysis

rates are computed by a DISORT four-stream implementation of the Tropospheric Ultraviolet Visible (TUV) radiative transfer code (Madronich and Flocke, 1998). These calculated profiles are then normalized to match the instantaneous observations at the time of measurement.

Model calculations use the 1-min merged data set available on the INTEX-B public data archive (<http://www-air.larc.nasa.gov>). In this study, we limit the analysis to those points that include direct measurement of NMHCs.

2.3 Photochemical steady-state

Due to the short lifetime of HO₂NO₂ with respect to thermal decomposition for the conditions experienced during the MILAGRO flights, photochemical steady state of HO₂NO₂ was assumed. To verify the validity of this assumption with respect to HO₂NO₂, the model was run in a non-steady state mode. A large, polluted perturbation was introduced into the model and allowed to decay over several days. A second set of calculations was performed in which each point was solved along the decay of the plume using steady state assumptions. While some species were not in equilibrium during this model run, the mixing ratios of HO₂NO₂ were consistent with the steady state run. This is attributed to the very short lifetime of HO₂NO₂ for the temperature range in the dataset. NO_x is directly input into the model while HO_x varies rapidly enough to represent the instantaneous precursor condition. At photochemical steady state, production and loss of HO₂NO₂ are equal and Reactions (R1–R3) yield (Kim et al., 2007):

$$[\text{HO}_2\text{NO}_2]_{\text{ss}} = \frac{k_1[\text{HO}_2][\text{NO}_2]}{J_2 + k_{-1} + k_3[\text{OH}]} \quad (1)$$

For the conditions experienced during the MILAGRO flights, the median lifetime of HO₂NO₂ with respect to thermal decomposition was five minutes while the lifetimes with respect to reaction with OH and UV/IR photolysis were on the order of 10 h and 6 days, respectively. Under these conditions, the steady-state concentration of HO₂NO₂ simplifies to:

$$[\text{HO}_2\text{NO}_2]_{\text{ss}} \approx \frac{k_1[\text{HO}_2][\text{NO}_2]}{k_{-1}} \quad (2)$$

To evaluate whether the simplified assumption for steady state (Eq. 2) is robust for MILAGRO conditions, NASA LaRC box model predictions of HO₂ and NO₂ were used in the right-hand side of Eq. (2) to calculate HO₂NO₂ using the steady state assumption ([HO₂NO₂]_{ss}). [HO₂NO₂]_{ss} was then compared to the full diurnal equilibrium model predictions of HO₂NO₂ (shown in Fig. 3). The slope of the robust fit line (DuMouchel and O'Brien, 1989; Street et al., 1988) is 1.02 and the intercept is 0.10 pptv. $R^2=0.99$.

The HO₂ mixing ratios measured from the C-130 were not sufficiently precise to provide for a direct comparison between the measurements of HO₂NO₂ and the steady state

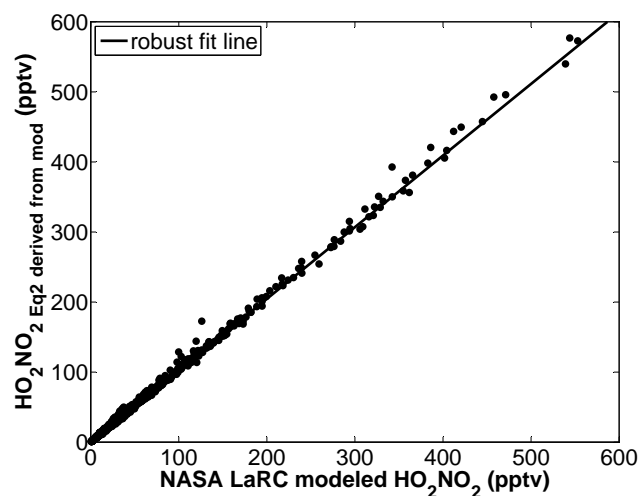


Fig. 3. [HO₂NO₂]_{ss}, calculated from Eq. (2), using modeled values of HO₂ and NO₂ versus HO₂NO₂ predicted by the NASA LaRC box model. The slope of the robust fit line is 1.02; intercept is 0.10 pptv; R^2 is 0.99, demonstrating that Eq. (2) is a valid simplification under MILAGRO conditions.

calculation of [HO₂NO₂]_{ss} using observed HO₂ and NO₂. However, the mean observed concentration of HO₂ was within 15% of the mean concentration of the NASA LaRC box model estimate for each of the flights used in this analysis.

3 Comparisons with NASA LaRC photochemical box model

An example time trace for HO₂NO₂ is illustrated in Fig. 4. During this flight (29 March 2006), the C-130 flew in and out of air masses heavily impacted by pollution from Mexico City. Variations in the measured and modeled HO₂NO₂ mixing ratio closely follow variations in NO₂.

Observed HO₂NO₂ mixing ratios, colored by NO_x mixing ratios, are compared to the NASA LaRC box model calculation of HO₂NO₂ mixing ratios in Fig. 5. The slope of the robust fit line is 0.81 and the intercept is 6.74 pptv. Although overall agreement is good ($R^2=0.82$), there is a tendency for the model to underpredict HO₂NO₂ concentrations at NO_x levels greater than 15 ppbv (shown by the red and orange colors in Fig. 5). Underprediction of HO₂NO₂ at elevated NO_x levels are in agreement with previous findings of Murphy et al. (2004) and Kim et al. (2007).

4 Ozone production

Photochemical ozone production is the result of oxidation of CO and hydrocarbons in reactions involving NO_x and HO_x.

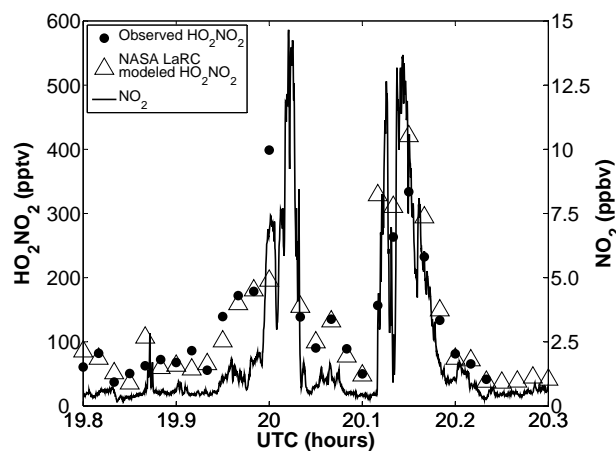


Fig. 4. Mixing ratios of HO₂NO₂ and NO₂ during Flight 29 March 2006 in an air mass heavily impacted by pollution. Dots are CIMS measurements of HO₂NO₂. Triangles are NASA LaRC box model values of HO₂NO₂. The solid line is observed NO₂ mixing ratio. Variations in the observed and modeled HO₂NO₂ mixing ratios closely follow variations in NO₂.

The instantaneous rate of photochemical ozone production can be calculated using Eq. (3) (Jacob, 1999).

$$P_{O_3} = k_{RO_2+NO}[RO_2][NO] + k_{HO_2+NO}[HO_2][NO] \quad (3)$$

The rate constants for the reactions of peroxyradicals (including HO₂) with NO are similar, so P_{O₃} can be approximated as:

$$P_{O_3} \approx k_{HO_2+NO}[NO]([RO_2] + [HO_2]) \quad (4)$$

In polluted atmospheres, HO₂ is produced primarily from the reaction of RO₂ with NO and therefore, the sum of all non-HO₂ peroxy radicals will be closely and linearly related to the concentration of HO₂ (e.g., Jacob, 1999).

$$P_{O_3} = Zk_{HO_2+NO}[HO_2][NO] \quad (5)$$

where Z is a number generally close to 2 in polluted air. With $K_{eq} = k_1/k_{-1}$, solving Eq. (2) for [HO₂] and substituting into Eq. (5) yields:

$$P_{O_3} = \frac{Zk_{HO_2+NO}[HO_2NO_2][NO]}{K_{eq}[NO_2]} \quad (6)$$

In Fig. 6, we plot P_{O₃} from the NASA LaRC box model versus $k_{HO_2+NO}[HO_2NO_2][NO]/K_{eq}[NO_2]$ to estimate Z. Using the NASA LaRC box model, we examined the predictions of Eq. (6). We limit this analysis to times when the solar zenith angle is <80°. The slope of the polyfit fit line, Z, in Fig. 6 is 1.77. The correlation is high ($R^2=0.99$) suggesting that the production of ozone under MILAGRO conditions can be estimated directly from Eq. (6) using measured HO₂NO₂, NO, and NO₂ with Z=1.77.

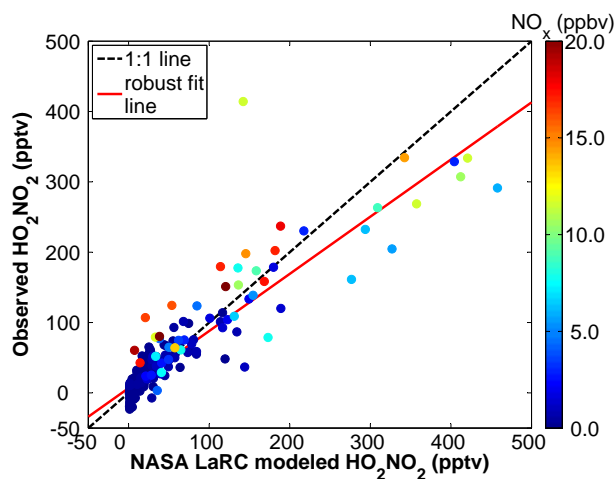
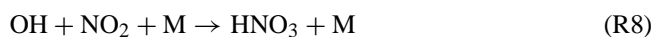


Fig. 5. Observed HO₂NO₂ versus NASA LaRC box model values of HO₂NO₂ colored by NO_x. The data presented are observed and modeled values at times when the model was constrained by NMHC observations. The slope of the robust fit line is 0.81; intercept is 6.74 pptv; R^2 is 0.82.

5 Discussion and conclusions

The rate of ozone production is sensitive to the rate of HO_x production and the amount of NO_x present. At a fixed HO_x production rate, the rate of ozone production increases with NO_x until NO_x reaches a level where the rate of nitric acid formation via Reaction (R8) reduces HO_x levels and photochemistry slows.



This behavior can be seen in the model chemistry (Fig. 7, middle panel). Ozone production rates for these MILAGRO flights calculated by the NASA LaRC box model are plotted versus NO levels and colored by the mixing ratio of CH₂O. CH₂O is used here as a proxy for the HO_x production rate (Seinfeld and Pandis, 2006). At low NO, the ozone production rate increases with NO at a fixed level of CH₂O, i.e., NO_x-limited behavior. At high NO, the ozone production rate becomes independent of or even decreases with NO at a fixed level of CH₂O, i.e., NO_x-saturated behavior.

In contrast to NASA LaRC box model calculations, the rate of ozone production estimated from observed HO₂NO₂, NO, and NO₂ does not show a saturation behavior (Fig. 7, left panel). At high NO, the rate of ozone production continues to increase with NO, in contrast to model predictions (Fig. 7, right panel). This suggests that the NASA LaRC box model underestimates the HO₂ levels and therefore either the HO_x production/loss rate is under/over estimated at elevated NO levels. This is consistent with observed HO₂NO₂ mixing ratios greater than NASA LaRC model predictions at NO_x levels greater than 15 ppbv shown in Fig. 5.

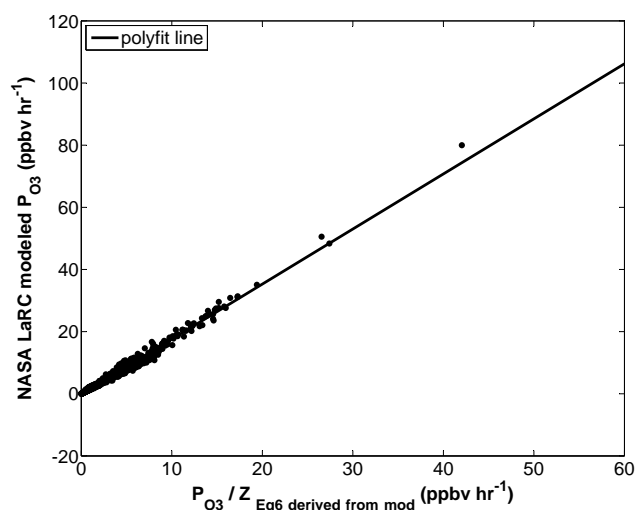


Fig. 6. The ozone production rate predicted by the NASA LaRC box model is compared to the rate of ozone production calculated using Eq. (6) and modeled values of HO₂NO₂, NO, and NO₂. The slope of the polyfit line, Z , is 1.77; R^2 is 0.99.

Observed values of HO₂NO₂, and hence HO₂, greater than those predicted by the NASA LaRC box model are consistent with a number of urban measurements of HO₂. Several recent studies have pointed to possible missing HO_x sources in urban air. At high NO_x concentrations, HO₂ levels calculated using highly constrained box models were significantly less than measured during summertime in Nashville, Birmingham, and New York City (Martinez et al., 2003; Heard et al., 2004; Emmerson et al., 2005; Ren et al., 2003) and in New York City and Tokyo in the winter (Ren et al., 2006; Kanaya et al., 2007). Martinez et al. (2003) reported daytime HO₂ levels 1.56 times modeled values in Nashville in 1999. The difference between measured and modeled HO₂ was positively correlated with high NO_x mixing ratios. In Birmingham, England in the summer of 1999 and winter of 2000, Heard et al. (2004) observed HO₂ levels 1.78 and 2.04 times modeled values, respectively. They found that the observed HO₂ concentrations were particularly insensitive to changes in NO_x levels. Summertime levels of HO₂ in New York City in 2001 were underestimated, with observed levels 1.24 times modeled values. The difference between measured and calculated HO₂ depended on the time of day. At midday, the observed and modeled values were found to agree very well while the model tended to underestimate the observations when NO_x was high, usually during the morning hours (Ren et al., 2003). Similar results were found in Tokyo during the winter of 2004. Daytime HO₂ concentrations were underestimated, with observed HO₂ levels 2.08 times modeled values. These comparisons were sensitive to the assumed hydrocarbon levels. When the concentrations of alkenes and reactive alkanes used in the model were in-

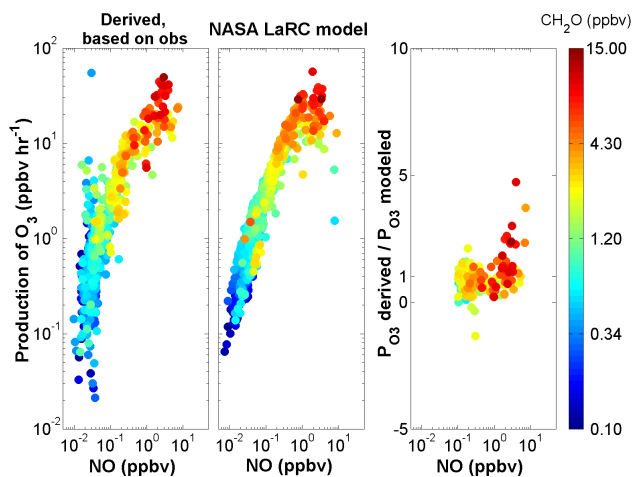


Fig. 7. P_{O₃} derived from Eq. (6) and based on measurements of HO₂NO₂ and NO_x versus observed NO, colored by observed CH₂O are shown in the left panel. NASA LaRC box model predictions of P_{O₃} versus modeled NO, colored by modeled CH₂O are shown in the middle panel. The ratio of derived P_{O₃}, based on measurements to NASA LaRC box model predictions of P_{O₃} for observed NO greater than 100 pptv, colored by observed CH₂O are shown in the right panel.

creased by factors of 3 and 5, respectively, the observed-to-modeled HO₂ ratio decreased to 1.13. Continued underestimation of HO₂ concentrations occurred at high NO_x mixing ratios (Kanaya et al., 2007). The higher than expected levels of HO₂ suggest higher rates of ozone production than can be accounted for using known chemistry.

It should be noted that the discrepancy between observed and modeled values of HO₂NO₂ at high NO_x found in this study appears to be distinct from the underprediction of HO_x values correlated with isoprene. Ren et al. (2008) found the observed-to-modeled OH ratio in the boundary layer to be strongly dependent on isoprene during the INTEX-NA summer 2004 campaign, with divergence occurring at isoprene levels greater than 100 pptv. Isoprene mixing ratios were well below 100 pptv for the vast majority of the data used in this analysis.

Not all studies have found excess HO₂. Indeed, several studies have found overpredictions of HO₂ levels by photochemical box models even at high NO_x concentrations. HO₂ concentrations were overestimated in the Los Angeles basin, Mexico City, and summertime Tokyo (George et al., 1999; Shirley et al., 2006; Kanaya et al., 2007). George et al. (1999) reported daytime HO₂ levels 0.67 times calculated values downwind of Los Angeles in 1993. The agreement of observed and calculated HO₂ was quite good in the early morning hours, but calculated HO₂ concentrations were found to be significantly higher than observations during midday. In Mexico City in 2003, Shirley et al. (2006) determined that observations of HO₂ were 0.79 times calculated values of

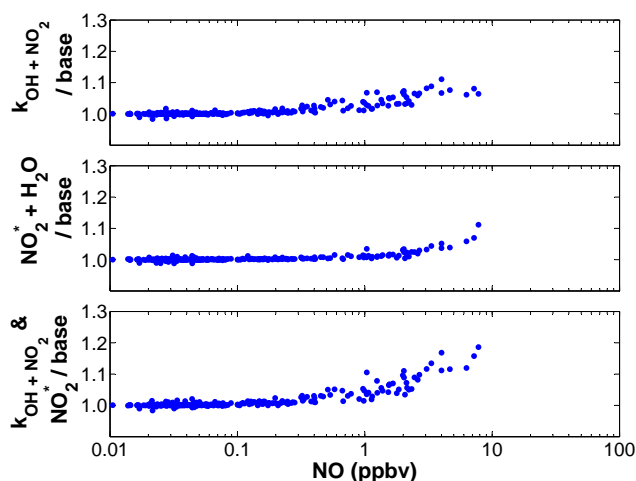


Fig. 8. Three different variations of the base model were investigated. The mixing ratio of HO₂NO₂ was calculated 1. using the 2000 JPL recommended rate constant for OH + NO₂, 2. including the reaction NO₂^{*} + H₂O → OH + HONO, and 3. using both the 2000 JPL recommended rate constant and the NO₂^{*} reaction. The y-axis is the ratio of HO₂NO₂ mixing ratio as calculated using a model variation to that calculated using the base model. Use of the 2000 JPL recommended rate constant for OH + NO₂ and inclusion of the NO₂^{*} + H₂O reaction result in higher HO₂NO₂ mixing ratios than calculated by the base model. This leads to better agreement between measured and calculated HO₂NO₂.

HO₂ during the midday. However, they also calculated an observed-to-modeled ratio of 1.17 during morning rush hour, coinciding with the morning rush hour peak in NO_x concentrations. Unlike wintertime findings, summertime HO₂ concentrations in Tokyo were overestimated. An observed-to-modeled HO₂ ratio of 0.78 was reported. Trends at high NO_x levels were not discussed as NO mixing ratios greater than 20 ppbv were not seen during this sampling period (Kanaya et al., 2007).

HO₂, HO₂NO₂, and hence the rate of ozone production may be underpredicted at high NO due to errors in calculated NO_x-dependent HO_x sources and sinks. We have investigated several possible sources of error. One possibility is an overestimate of the rate constant of Reaction (R8), a sink of HO_x. The accepted rate constant for Reaction (R8) has been subject to numerous revisions in the last decade (DeMore et al., 1997; Sander et al., 2000, 2003, 2006). In addition, a recommended rate constant for the reaction of OH and NO₂ to form pernitrous acid (HOONO) is included for the first time in the 2006 JPL critical evaluation. Recent laboratory work at Jet Propulsion Laboratory and California Institute of Technology suggests that the 2000 JPL critical evaluation recommendation (Sander et al., 2000) may be closer to the true rate of Reaction (R8) (Okumura and Sander, 2005) than the current recommendation (Sander et al., 2006). The 2000 JPL critical evaluation recommended rate constant for Reac-

tion (R8) is approximately 30% lower for MILAGRO conditions than the current evaluation. The explicit rate constant for HNO₃ formation was used in the model. The model does not include the HOONO branch of the OH+NO₂+M reaction due to the short lifetime (seconds to minutes) of HOONO under MILAGRO conditions. The formation and breakdown of HOONO is considered to be a null cycle under these conditions (Fry et al., 2004). A reduction in the rate constant for Reaction (R8) leads to an increase in OH and NO₂ mixing ratios, leading to an increase in HO₂NO₂ levels. To test the importance of this modified rate constant on HO₂NO₂ levels, the 2000 JPL critical evaluation recommended rate constant for Reaction (R8) was substituted into the model. Figure 8 (top panel) illustrates the sensitivity of the modeled HO₂NO₂ mixing ratio to a change in the rate constant for Reaction (R8). At high NO levels, use of the 2000 JPL recommended rate constant increases the mixing ratio of calculated HO₂NO₂, leading to better agreement between measured and calculated HO₂NO₂.

HO₂NO₂ mixing ratios and hence rate of ozone production may also be underpredicted at high NO_x due to missing calculated HO_x sources at high NO_x. Li et al. (2008) recently reported significant HO_x production from the reaction of excited-state NO₂ (NO₂^{*}) with H₂O:



NO₂^{*} is formed through the excitation of NO₂ at wavelengths longer than 420 nm. These direct and indirect (via HONO photolysis) OH sources lead to increased concentrations of HO_x at elevated NO_x levels. Including this process in the box model, using the rate of Reaction (R9) determined by Li et al., improves agreement with observed HO₂NO₂. As seen in Fig. 8 (middle panel), the inclusion of Reaction (R9) increases the mixing ratio of modeled HO₂NO₂, again leading to better agreement between measured and modeled HO₂NO₂. Including both the reduced rate of Reaction (R8) and the Li et al. (2008) process leads to increased levels of modeled HO₂NO₂ (Fig. 8, bottom panel). Increased levels of calculated HO₂NO₂ are in better agreement with observations. These two recently suggested ideas lead to better, not perfect, agreement between observed and calculated HO₂NO₂.

The transition to NO_x saturation appears to occur at higher NO_x levels than estimated by the NASA LaRC box model for Mexico City. This may have implications for engineering of improvements in air quality in the basin. If generally true, it suggests that further NO_x controls will yield reductions in smog levels. Significant uncertainties remain, however. It is unclear why the HO_x levels are generally underestimated. Although we identify several possible deficiencies in the photochemical mechanism that may contribute to an underprediction of HO_x, these are not sufficient to account for the discrepancy and each is uncertain and requires additional laboratory work to test these mechanisms (e.g., Wennberg

and Dabdub, 2008). In addition, NO_x levels are generally much higher at the surface and so it is unclear if NO_x-limited conditions also apply.

Acknowledgements. The authors wish to thank C. M. Roehl for synthesizing the peroxyxynitric acid for calibration. P. Weibring and A. Fried, D. R. Blake, and R. E. Shetter provided formaldehyde, whole air sample, and solar actinic flux measurements, respectively, which provided constraints for the photochemical box model. The authors also wish to thank the C-130 crew and support team. The HO₂NO₂ measurements and their interpretation was made possible with the financial support of NASA (NAG: NNG06GB32B). J. D. C. acknowledges support from the EPA-STAR Fellowship Program (FP916334012). This work has not been formally reviewed by the EPA. The views expressed in this document are solely those of the authors and the EPA does not endorse any products or commercial services mentioned in this publication.

Edited by: S. Madronich

References

- Amelynck, C., Schoon, N., and Arijis, E.: Gas phase reactions of CF₃O⁻ and CF₃O⁻·H₂O with nitric, formic, and acetic acid, *Int. J. Mass Spectrom.*, 203, 165–175, 2000.
- Amelynck, C., Van Bavel, A. M., Schoon, N., and Arijis, E.: Gas phase reactions of CF₃O⁻ and CF₃O⁻·H₂O and their relevance to the detection of stratospheric HCl, *Int. J. Mass Spectrom.*, 202, 207–216, 2000.
- Arnold, S. R., Chipperfield, M. P., and Blitz, M. A.: A three-dimensional model study of the effect of new temperature-dependent quantum yields for acetone photolysis, *J. Geophys. Res.-Atmos.*, 110, D22305, doi:10.1029/2005JD005998, 2005.
- Atkinson, R., Baulch, D. L., Cox, R. A., Crowley, J. N., Hampson, R. F., Hynes, R. G., Jenkin, M. E., Rossi, M. J., and Troe, J.: Evaluated kinetic and photochemical data for atmospheric chemistry: Volume I – gas phase reactions of O_x, HO_x, NO_x and SO_x species, *Atmos. Chem. Phys.*, 4, 1461–1738, 2004, <http://www.atmos-chem-phys.net/4/1461/2004/>.
- Barnes, I., Bastian, V., Becker, K. H., Fink, E. H., and Zabel, F.: Pressure Dependence of the Reaction of OH with HO₂NO₂, *Chem. Phys. Lett.*, 123, 28–32, 1986.
- Blake, N. J., Blake, D. R., Simpson, I. J., Meinardi, S., Swanson, A. L., Lopez, J. P., Katzenstein, A. S., Barletta, B., Shirai, T., Atlas, E., Sachse, G., Avery, M., Vay, S., Fuelberg, H. E., Kiley, C. M., Kita, K., and Rowland, F. S.: NMHCs and halocarbons in Asian continental outflow during the Transport and Chemical Evolution over the Pacific (TRACE-P) Field Campaign: Comparison with PEM-West B, *J. Geophys. Res.-Atmos.*, 108, 8806, doi:10.1029/2002JD003367, 2003.
- Campos, T. L., Weinheimer, A. J., Zheng, J., Montzka, D. D., Walega, J. G., Grahek, F. E., Vay, S. A., Collins, J. E., Wade, L. O., Sachse, G. W., Anderson, B. E., Brune, W. H., Tan, D., Faloon, I., Baughcum, S. L., and Ridley, B. A.: Measurement of NO and NO_y emission indices during SUCCESS, *Geophys. Res. Lett.*, 25, 1713–1716, 1998.
- Cantrell, C. A., Edwards, G. D., Stephens, S., Mauldin, L., Kosciuch, E., Zondlo, M., and Eisele, F.: Peroxy radical observations using chemical ionization mass spectrometry during TOPSE, *J. Geophys. Res.-Atmos.*, 108, 8371, doi:10.1029/2002JD002715, 2003.
- Colman, J. J., Swanson, A. L., Meinardi, S., Sive, B. C., Blake, D. R., and Rowland, F. S.: Description of the analysis of a wide range of volatile organic compounds in whole air samples collected during PEM-Tropics A and B, *Anal. Chem.*, 73, 3723–3731, 2001.
- Crouse, J. D., McKinney, K. A., Kwan, A. J., and Wennberg, P. O.: Measurement of gas-phase hydroperoxides by chemical ionization mass spectrometry, *Anal. Chem.*, 78, 6726–6732, 2006.
- DeMore, W. B., Sander, S. P., Golden, D. M., Hampson, R. F., Kurylo, M. J., Howard, C. J., Ravishankara, A. R., Kolb, C. E., and Molina, M. J.: Chemical Kinetics and Photochemical Data for Use in Stratospheric Modeling, Evaluation Number 12, JPL Publication 97-4, NASA Jet Propulsion Laboratory, California Institute of Technology, Pasadena, CA 1997.
- DuMouchel, W. H. and O'Brien, F. L.: Integrating a Robust Option into a Multiple Regression Computing Environment, *Computer Science and Statistics: Proceedings of the 21st Symposium on the Interface*, Alexandria, VA, American Statistical Association, 1989.
- Emmerson, K. M., Carslaw, N., Carpenter, L. J., Heard, D. E., Lee, J. D., and Pilling, M. J.: Urban atmospheric chemistry during the PUMA campaign 1: Comparison of modelled OH and HO₂ concentrations with measurements, *J. Atmos. Chem.*, 52, 143–164, 2005.
- Fried, A., Crawford, J., Olson, J., Walega, J., Potter, W., Wert, B., Jordan, C., Anderson, B., Shetter, R., Lefer, B., Blake, D., Blake, N., Meinardi, S., Heikes, B., O'Sullivan, D., Snow, J., Fuelberg, H., Kiley, C. M., Sandholm, S., Tan, D., Sachse, G., Singh, H., Faloon, I., Harward, C. N., and Carmichael, G. R.: Airborne tunable diode laser measurements of formaldehyde during TRACE-P: Distributions and box model comparisons, *J. Geophys. Res.-Atmos.*, 108, 8798, doi:10.1029/2003JD003451, 2003.
- Frost, G. J., Fried, A., Lee, Y. N., Wert, B., Henry, B., Drummond, J. R., Evans, M. J., Fehsenfeld, F. C., Goldan, P. D., Holloway, J. S., Hubler, G., Jakoubek, R., Jobson, B. T., Knapp, K., Kuster, W. C., Roberts, J., Rudolph, J., Ryerson, T. B., Stohl, A., Stroud, C., Sueper, D. T., Trainer, M., and Williams, J.: Comparisons of box model calculations and measurements of formaldehyde from the 1997 North Atlantic Regional Experiment, *J. Geophys. Res.-Atmos.*, 107, 4060, doi:10.1029/2001JD000896, 2002.
- Fry, J. L., Nizkorodov, S. A., Okumura, M., Roehl, C. M., Francisco, J. S., and Wennberg, P. O.: Cis-cis and trans-perp HOONO: Action spectroscopy and isomerization kinetics, *J. Chem. Phys.*, 121, 1432–1448, 2004.
- George, L. A., Hard, T. M., and O'Brien, R. J.: Measurement of free radicals OH and HO₂ in Los Angeles smog, *J. Geophys. Res.-Atmos.*, 104, 11643–11655, 1999.
- Gierczak, T., Jimenez, E., Riffault, V., Burkholder, J. B., and Ravishankara, A. R.: Thermal Decomposition of HO₂NO₂ (Peroxyxynitric Acid, PNA): Rate Coefficient and Determination of the Enthalpy of Formation, *J. Phys. Chem. A.*, 109, 586–596, 2005.
- Graham, R. A., Winer, A. M., and Pitts, J. N.: Temperature dependence of the unimolecular decomposition of pernitric acid and its atmospheric implications, *Chem. Phys. Lett.*, 51, 215–220, 1977.
- Graham, R. A., Winer, A. M., and Pitts, J. N.: Pressure and Temperature Dependence of Unimolecular Decomposition of HO₂NO₂,

- J. Chem. Phys., 68, 4505–4510, 1978.
- Heard, D. E., Carpenter, L. J., Creasey, D. J., Hopkins, J. R., Lee, J. D., Lewis, A. C., Pilling, M. J., Seakins, P. W., Carslaw, N., and Emmerson, K. M.: High levels of the hydroxyl radical in the winter urban troposphere, *Geophys. Res. Lett.* 31, L18112, doi:10.1029/2004GL020544, 2004.
- Huey, L. G., Hanson, D. R., and Howard, C. J.: Reactions of SF₆⁻ and I⁻ with atmospheric trace gases, *J. Phys. Chem.*, 99, 5001–5008, 1995.
- Huey, L. G., Villalta, P. W., Dunlea, E. J., Hanson, D. R., and Howard, C. J.: Reactions of CF₃O⁻ with atmospheric trace gases, *J. Phys. Chem.*, 100, 190–194, 1996.
- Jacob, D. J.: *Introduction to Atmospheric Chemistry*, Princeton University Press, 1999.
- Jaegle, L., Jacob, D. J., Brune, W. H., Faloon, I., Tan, D., Heikes, B. G., Kondo, Y., Sachse, G. W., Anderson, B., Gregory, G. L., Singh, H. B., Poeschel, R., Ferry, G., Blake, D. R., and Shetter, R. E.: Photochemistry of HO_x in the upper troposphere at northern midlatitudes, *J. Geophys. Res.-Atmos.*, 105, 3877–3892, 2000.
- Jimenez, E., Gierczak, T., Stark, H., Burkholder, J. B., and Ravishankara, A. R.: Reaction of OH with HO₂NO₂ (Peroxynitric Acid): Rate Coefficients between 218 and 335 K and Product Yields at 298 K, *J. Phys. Chem. A.*, 108, 1139–1149, 2004.
- Kanaya, Y., Cao, R. Q., Akimoto, H., Fukuda, M., Komazaki, Y., Yokouchi, Y., Koike, M., Tanimoto, H., Takegawa, N., and Kondo, Y.: Urban photochemistry in central Tokyo: 1. Observed and modeled OH and HO₂ radical concentrations during the winter and summer of 2004, *J. Geophys. Res.-Atmos.*, 112, D21312 doi:10.1029/2007JD008670, 2007.
- Kim, S., Huey, L. G., Stickel, R. E., Tanner, D. J., Crawford, J. H., Olson, J. R., Chen, G., Brune, W. H., Ren, X., Leshner, R., Wooldridge, P. J., Bertram, T. H., Perring, A., Cohen, R. C., Lefler, B. L., Shetter, R. E., Avery, M., Diskin, G., and Sokolik, I.: Measurement of HO₂NO₂ in the free troposphere during the intercontinental chemical transport experiment – North America 2004, *J. Geophys. Res.-Atmos.*, 112, D12S01, doi:10.1029/2006JD007676, 2007.
- Knight, G., Ravishankara, A. R., and Burkholder, J. B.: UV absorption cross sections of HO₂NO₂ between 343 and 273 K, *Phys. Chem. Chem. Phys.*, 4, 1432–1437, 2002.
- Li, S. P., Matthews, J., and Sinha, A.: Atmospheric hydroxyl radical production from electronically excited NO₂ and H₂O, *Science*, 319, 1657–1660, 2008.
- Lurmann, F. W., Lloyd, A. C., and Atkinson, R.: A Chemical Mechanism for Use in Long-Range Transport Acid Deposition Computer Modeling, *J. Geophys. Res.-Atmos.*, 91, 10905–10936, 1986.
- Macleod, H., Smith, G. P., and Golden, D. M.: Photodissociation of Peroxynitric Acid (HO₂NO₂) at 248 nm, *J. Geophys. Res.-Atmos.*, 93, 3813–3823, 1988.
- Madronich, S. and Flocke, S.: The role of solar radiation in atmospheric chemistry, in: *Handbook of Environmental Chemistry*, edited by: Boule, P., Springer, 1–26, 1998.
- Martinez, M., Harder, H., Kovacs, T. A., Simpas, J. B., Bassis, J., Leshner, R., Brune, W. H., Frost, G. J., Williams, E. J., Stroud, C. A., Jobson, B. T., Roberts, J. M., Hall, S. R., Shetter, R. E., Wert, B., Fried, A., Alicke, B., Stutz, J., Young, V. L., White, A. B., and Zamora, R. J.: OH and HO₂ concentrations, sources, and loss rates during the Southern Oxidants Study in Nashville, Tennessee, Summer 1999, *J. Geophys. Res.-Atmos.*, 108, D194617, doi:10.1029/2003JD003551, 2003.
- Miller, E. R. and R. B. Friesen: Standard output data products from the NCAR Research Aviation Facility, NCAR RAF Bulletin 9, <http://www.eol.ucar.edu/raf/Bulletins/bulletin9.html>, 1985.
- Murphy, J. G., Thornton, J. A., Wooldridge, P. J., Day, D. A., Rosen, R. S., Cantrell, C., Shetter, R. E., Lefler, B., and Cohen, R. C.: Measurements of the sum of HO₂NO₂ and CH₃O₂NO₂ in the remote troposphere, *Atmos. Chem. Phys.*, 4, 377–384, 2004, <http://www.atmos-chem-phys.net/4/377/2004/>.
- Niki, H., Maker, P. D., Savage, C. M., and Breitenbach, L. P.: Fourier transform IR spectroscopic observation of pernitric acid formed via HOO + NO₂ → HOONO₂, *Chem. Phys. Lett.*, 45, 564–566, 1977.
- Olson, J. R., Crawford, J. H., Chen, G., Fried, A., Evans, M. J., Jordan, C. E., Sandholm, S. T., Davis, D. D., Anderson, B. E., Avery, M. A., Barrick, J. D., Blake, D. R., Brune, W. H., Eisele, F. L., Flocke, F., Harder, H., Jacob, D. J., Kondo, Y., Lefler, B. L., Martinez, M., Mauldin, R. L., Sachse, G. W., Shetter, R. E., Singh, H. B., Talbot, R. W., and Tan, D.: Testing fast photochemical theory during TRACE-P based on measurements of OH, HO₂, and CH₂O, *J. Geophys. Res.-Atmos.*, 109, D15S10, doi:10.1029/2003JD004278, 2004.
- Olson, J. R., Crawford, J. H., Chen, G., Brune, W. H., Faloon, I. C., Tan, D., Harder, H., and Martinez, M.: A reevaluation of airborne HO_x observations from NASA field campaigns, *J. Geophys. Res.-Atmos.*, 111, D10301, doi:10.1029/2005JD006617, 2006.
- Okumura, M. and Sander, S. P.: Gas-Phase Formation Rates of Nitric Acid and its Isomers under Urban Conditions, State of California Air Resources Board, 2005.
- Ravishankara, A. R., Dunlea, E. J., Blitz, M. A., Dillon, T. J., Heard, D. E., Pilling, M. J., Strekowski, R. S., Nicovich, J. M., and Wine, P. H.: Redetermination of the rate coefficient for the reaction of O(¹D) with N₂, *Geophys. Res. Lett.*, 29, 1745, doi:10.1029/2002GL014850, 2002.
- Ren, X. R., Harder, H., Martinez, M., Leshner, R. L., Olinger, A., Simpas, J. B., Brune, W. H., Schwab, J. J., Demerjian, K. L., He, Y., Zhou, X. L., and Gao, H. G.: OH and HO₂ chemistry in the urban atmosphere of New York City, *Atmos. Environ.*, 37, 3639–3651, 2003.
- Ren, X. R., Brune, W. H., Mao, J. Q., Mitchell, M. J., Leshner, R. L., Simpas, J. B., Metcalf, A. R., Schwab, J. J., Cai, C. X., Li, Y. Q., Demerjian, K. L., Felton, H. D., Boynton, G., Adams, A., Perry, J., He, Y., Zhou, X. L., and Hou, J.: Behavior of OH and HO₂ in the winter atmosphere in New York City, *Atmos. Environ.*, 40, S252–S263, 2006.
- Ren, X. R., Olson, J. R., Crawford, J. H., Brune, W. H., Mao, J. Q., Long, R. B., Chen, Z., Chen, G., Avery, M. A., Sachse, G. W., Barrick, J. D., Diskin, G. S., Huey, L. G., Fried, A., Cohen, R. C., Heikes, B., Wennberg, P. O., Singh, H. B., Blake, D. R., and Shetter, R. E.: HO_x chemistry during INTEX-A 2004: Observation, model calculation, and comparison with previous studies, *J. Geophys. Res.-Atmos.*, 113, D05310, doi:10.1029/2007JD009166, 2008.
- Roehl, C. M., Nizkorodov, S. A., Zhang, H., Blake, G. A., and Wennberg, P. O.: Photodissociation of Peroxynitric Acid in the Near-IR, *J. Phys. Chem. A.*, 106, 3766–3772, 2002.

- Rothman, L. S., Jacquemart, D., Barbe, A., Benner, D. C., Birk, M., Brown, L. R., Carleer, M. R., Chackerian, C., Chance, K., Coudert, L. H., Dana, V., Devi, V. M., Flaud, J. M., Gamache, R. R., Goldman, A., Hartmann, J. M., Jucks, K. W., Maki, A. G., Mandin, J. Y., Massie, S. T., Orphal, J., Perrin, A., Rinsland, C. P., Smith, M. A. H., Tennyson, J., Tolchenov, R. N., Toth, R. A., Vander Auwera, J., Varanasi, P., and Wagner, G.: The HITRAN 2004 molecular spectroscopic database, *J. Quant. Spectrosc. Ra.*, 96, 139–204, 2005.
- Sander, S. P., Friedl, R. R., DeMore, W. B., Golden, D. M., Kurylo, M. J., Hampson, R. F., Huie, R. E., Moortgat, G. K., Ravishankara, A. R., Kolb, C. E., and Molina, M. J.: Chemical Kinetics and Photochemical Data for Use in Stratospheric Modeling Supplement to Evaluation 12: Update of Key Reactions, JPL Publication 00-3, NASA Jet Propulsion Laboratory, California Institute of Technology, Pasadena, CA, 2000.
- Sander, S. P., Friedl, R. R., Golden, D. M., Kurylo, M. J., Huie, R. E., Orkin, V. L., Moortgat, G. K., Ravishankara, A. R., Kolb, C. E., Molina, M. J., and Finlayson-Pitts, B. J.: Chemical Kinetics and Photochemical Data for Use in Atmospheric Studies, Evaluation Number 14 JPL Publication 02-25, NASA Jet Propulsion Laboratory, California Institute of Technology, Pasadena, CA, 2003.
- Sander, S. P., Friedl, R. R., Golden, D. M., Kurylo, M. J., Moortgat, G. K., Keller-Rudek, H., Wine, P. H., Ravishankara, A. R., Kolb, C. E., Molina, M. J., Finlayson-Pitts, B. J., Huie, R. E., and Orkin, V. L.: Chemical Kinetics and Photochemical Data for Use in Atmospheric Studies, Evaluation Number 15 JPL Publication 06-2, NASA Jet Propulsion Laboratory, California Institute of Technology, Pasadena, CA, 2006.
- Seinfeld, J. H. and Pandis, S. N.: *Atmospheric Chemistry and Physics*, 2nd ed., John Wiley & Sons, Inc., 2006.
- Shetter, R. E. and Muller, M.: Photolysis frequency measurements using actinic flux spectroradiometry during the PEM-Tropics mission: Instrumentation description and some results, *J. Geophys. Res.-Atmos.*, 104, 5647–5661, 1999.
- Shirley, T. R., Brune, W. H., Ren, X., Mao, J., Leshner, R., Cardenas, B., Volkamer, R., Molina, L. T., Molina, M. J., Lamb, B., Velasco, E., Jobson, T., and Alexander, M.: Atmospheric oxidation in the Mexico City Metropolitan Area (MCMA) during April 2003, *Atmos. Chem. Phys.*, 6, 2753–2765, 2006, <http://www.atmos-chem-phys.net/6/2753/2006/>.
- Slusher, D. L., Pitteri, S. J., Haman, B. J., Tanner, D. J., and Huey, L. G.: A chemical ionization technique for measurement of per-nitric acid in the upper troposphere and the polar boundary layer, *Geophys. Res. Lett.*, 28, 3875–3878, 2001.
- Smith, C. A., Molina, L. T., Lamb, J. J., and Molina, M. J.: Kinetics of the Reaction of OH with Pernitric and Nitric Acids, *Int. J. Chem. Kin.*, 16, 41–55, 1984.
- Street, J. O., Carroll, R. J., and Ruppert, D.: A Note on Computing Robust Regression Estimates via Iteratively Reweighted Least Squares, *The American Statistician*, 42, 152–154, 1988.
- Trevor, P. L., Black, G., and Barker, J. R.: Reaction Rate Constant for OH + HOONO₂ → Products over the Temperature Range 246 to 324 K, *J. Phys. Chem.*, 86, 1661–1669, 1982.
- Weinheimer, A. J., Montzka, D. D., Campos, T. L., Walega, J. G., Ridley, B. A., Donnelly, S. G., Keim, E. R., Del Negro, L. A., Proffitt, M. H., Margitan, J. J., Boering, K. A., Andrews, A. E., Daube, B. C., Wofsy, S. C., Anderson, B. E., Collins, J. E., Sachse, G. W., Vay, S. A., Elkins, J. W., Wamsley, P. R., Atlas, E. L., Flocke, F., Schauffler, S., Webster, C. R., May, R. D., Loewenstein, M., Podolske, J. R., Bui, T. P., Chan, K. R., Bowen, S. W., Schoeberl, M. R., Lait, L. R., and Newman, P. A.: Comparison between DC-8 and ER-2 species measurements in the tropical middle troposphere: NO, NO_y, O₃, CO₂, CH₄, and N₂O, *J. Geophys. Res.-Atmos.*, 103, 22087–22096, 1998.
- Wennberg, P. O. and Dabdub, D.: Atmospheric chemistry – Re-thinking ozone production, *Science*, 319, 1624–1625, 2008.
- Wert, B. P., Fried, A., Rauenbuehler, S., Walega, J., and Henry, B.: Design and performance of a tunable diode laser absorption spectrometer for airborne formaldehyde measurements, *J. Geophys. Res.-Atmos.*, 108, 4350 doi:10.1029/2002JD002872, 2003.
- Zabel, F.: Unimolecular Decomposition of Peroxynitrates, *Zeitschrift für Physikalische Chemie-International, Journal of Research in Physical Chemistry & Chemical Physics*, 188, 119–142, 1995.